Tailoring agrichemical release kinetics through material design: Understanding the counterintuitive effect of matrix hydrophobicity

Ian Levett [a], Minjie Liao [a], Chris Pratt [b], Matthew Redding [c], Steven Pratt [a], Bronwyn Laycock [a,*]

[a] School of Chemical Engineering, University of Queensland, QLD, 4072, Australia
[b] School of Environment and Science/Australian Rivers Institute, Griffith University, Australia
[c] Department of Primary Industries (DPI), Toowoomba, QLD, 4350, Australia

ARTICLE INFO

ABSTRACT

Nitrification inhibitors (NIs), such as dicyandiamide (DCD), can improve the nitrogen uptake efficiency by plants and reduce environmental losses. Unfortunately, DCD degrades rapidly through microbial action in tropical conditions, limiting its efficacy. Here, the encapsulation and controlled release of DCD as a model water-soluble, crystalline agrichemical was studied within biodegradable matrices comprising blends of poly(3-hydroxybutyrate-*co*-3-hydroxyvalerate) (PHBV) and poly(ε-caprolactone) (PCL). DCD was mixed at 40 wt% and extruded with PHBV:PCL blends at polymer mass ratios of 1:0, 3:1, 1:1, 1:3 and 0:1 to produce ~3 × 3 mm cylindrical pellets. The release kinetics into water were monitored over 12 weeks at 10, 23 and 40 °C. A Fickian diffusion model fitted the data well and the diffusivities followed an Arrhenius dependence on temperature. Counterintuitively, the more hydrophobic PHBV matrix released DCD the fastest. Release kinetics slowed as the PCL content increased, except for the neat PCL matrix. The lower affinity between the hydrophobic PHBV and hydrophilic DCD led to the DCD being relatively excluded from the PHBV phase and hence more accessible to interconnected voids and channels. In contrast, the higher affinity between PCL and DCD led to PCL-coated DCD crystals, which reduced direct water access to the DCD. Therefore, as the content of PCL was increased, the layer of PCL through which water and dissolved DCD must diffuse also increased, slowing release. This work demonstrated the ability to control DCD release from a biopolymer matrix through material design, with complete release taking between a few days to several months depending on the blend ratio.

1. Introduction

Globally, environmental losses of fertiliser-derived nitrogen (N) are so significant that they are classified as being at high risk of destabilizing the Earth system [1]. One approach to minimize N losses from agricultural fields is the use of nitrification inhibitors (NIs). These chemicals, such as dicyandiamide (DCD), 3,4-dimethyl-1H-pyrazole phosphate (DMPP) and 2-chloro-6-(trichloromethyl)-pyridine (nitrapyrin), bind to the bacterial membrane-bound ammonium monooxygenase (AMO) enzyme. This enzyme is responsible for the rapid oxidation of ammonium to nitrate in soil following amendment with ammonium or urea-based N fertilisers. The high concentration of nitrate is then vulnerable to direct leaching and runoff during irrigation and rainfall events, and also gaseous emissions, through denitrification to nitrous oxide (N_2O) and nitric oxide (NO) [2]. Deactivating AMO with NIs has been shown to be effective at reducing all these N loss pathways [3–5]. The

low cost of NIs compared to controlled release fertilisers offers agronomic benefits for broad acre agriculture. However, NIs degrade in soil at rates that increase exponentially with soil temperature [6,7], limiting their efficacy in tropical agriculture. The encapsulation and slow release could protect the encapsulated inhibitor from degradation, through shielding it from soil microbes, thereby extending the duration of an effective concentration in the soil and thus increasing the overall efficacy of a given equivalent dose. Additionally, water driven losses of the NI can be mitigated, since the NI is encapsulated and therefore cannot be leached from the soil with irrigation or rainwater. An additional benefit of slowly releasing the NIs is to mitigate against potential toxic affects they can have on soil microbiota [8], grazing animals [9], adjacent aquatic ecosystems [10] and even to the crop itself [11]. By reducing the initial loading of the NI and slowly releasing them into the soil profile, it is likely to reduce the exposure level of the inhibitors for off-target organisms.

DCD is used here as a model NI that is effective in temperate climates [5], low cost, and widely available, but also because its degradation has been extensively studied. Kelliher, Clough [12] collated literature data on the degradation of DCD, showing that the half-life of DCD declines exponentially with increasing soil temperature, from ~120 days at 10 °C to ~20 days above 20 °C. The high sensitivity of DCD longevity to soil temperature means it could benefit significantly from a controlled-release system to improve its efficacy in tropical soils. However, the knowledge gained in this study should aid the development of controlled-release systems for any water-soluble crystalline compound.

In terms of the selection of polymer matrix for encapsulation, we have chosen to only use soil biodegradable options. There are several commercially available slow- and controlled-release agrichemical products that utilize polymers that degrade very slowly in the soil. Polymers such as polyethylene and other polyolefins, polyurethanes and synthetic rubbers will accumulate in the soil and can form persistent hazardous micro-plastics [13]. Here, we propose the use of fully biodegradable blends of poly(3-hydroxybutyrate-*co*-3-hydroxyvalerate) (PHBV) and poly(ε-caprolactone) (PCL) as matrices to control the release of DCD. Both polymers degrade through slow hydrolysis of ester linkages, catalyzed by soil microbial enzymes and completely degrade to carbon dioxide, biomass and water [14]. In our previous works [15,16], controlled release DCD pellets were successfully produced through extrusion with PHBV. By varying the loading of DCD within the PHBV matrix the percolation threshold (that is, the loading at which a complete interconnected network of DCD crystals forms) was found to lie between 20 wt% DCD and 40 wt% DCD, independent of the particle size of the DCD powder [16]. However, below the percolation threshold, the DCD particle size significantly altered the proportion of surface exposed DCD, allowing control over the degree of "burst" release (release within the first 24 h in water). At 20 wt% DCD loading, the fractional release after 24 h was 7.3 %, 27.0 %, and 49 % for DCD crystals size fractions of 0–106 μm, 106–250 μm and > 250 μm, respectively.

The present study extends this knowledge, to explore the impact of incorporating an alternative biodegradable polymer, PCL, with dramatically different properties to PHBV. Table 1 summarises the key properties, molecular structure, Hildebrand solubility parameter (δ_T) and water diffusivity (D_w) of each polymer. Both polymers were selected for their biodegradability, hydrophobicity and ease of melt processing. Both are semi-crystalline linear aliphatic polyester thermoplastics. PHBV is a natural polyester belonging to the family of poly-hydroxyalkanoates (PHAs) that are synthesized by numerous bacteria for intracellular carbon storage, with low HV content PHBV typically being strong (30–40 MPa), but brittle (<5 % elongation at break) [17]. In contrast, PCL is a synthetic polymer, derived from the ring opening polymerization of ε-caprolactone, with more elastomeric properties, yielding at 13 MPa with a strain of 20 %, but continuing to stretch until ~600–700 % elongation at break [18]. Both polymers are described as

being hydrophobic, with similar water contact angles around 85–90° (Table 1). However, the higher δ_T of PHBV indicates higher hydrophobicity over PCL. Additionally, water permeates through PCL films an order of magnitude faster than through PHBV films as indicated in Table 1, with D_w of PHBV being ~15 times lower than that of PCL [19]. Blending these polymers leads to the formation of a phase separated polymer matrix, the structure of which depends on the blend ratio [20,21]. Blends with significantly more of one component tend to form a continuous phase of the dominating polymer with isolated "islands" of the secondary polymer, while at intermediate blend ratios a co-continuous structure can arise [22]. The architecture of the phase separated structure can alter the pathways through which water and water-soluble compounds migrate through the polymer matrix. The dramatically different thermal and physiochemical properties of the two polymers is the basis of the present work, assuming they will exhibit dramatically different rates of DCD release, and manipulating the blend composition could be a method to match release rates to a desired delivery timeframe.

The use of PHBV/PCL blends has been demonstrated in the literature to effectively control the release of agrichemicals, such as fertilisers [27], herbicides [28], pesticides [29] and various orally administered drugs [30–32]. These studies show that the differences in chemical and physical properties between PHBV and PCL could allow control over the release kinetics when blended in different ratios. Cold pressing PHBV/PCL blends with agrichemicals such as ammonium nitrate fertiliser [27] or metribuzin herbicide [28] is a simple method to produce controlled release pellets. Surprisingly, these studies showed different impacts of incorporating PCL in the formulation even with the same agrichemical loading of 25 wt% and the same production method. Boyandin, Kazantseva [27], for example, showed essentially no impact on release kinetics in soil with incorporation of PCL. In contrast, Boyandin, Zhila [28] showed that a 70/30 P3HB/PCL blend slowed the release of metribuzin from 35% release after 35 days for neat P3HB to 17 % release for the blend. Suave, Dall'Agnol [29] showed that PCL incorporation can accelerate release for malathion loaded into microspheres containing blends of P3HB and PCL, with the faster release occurring for 80/20 and 70/30 P3HB/PCL blends. From these studies, there remains a lack of clarity around the impact of blending PCL with PHBV on the release kinetics of active agents encapsulated within the blend, and the underlying transport mechanisms.
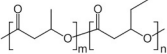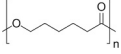
This work aims to explore the potential of blending these two contrasting polymers to control the release of the nitrification inhibitor, DCD. It was anticipated that the morphology of the phase separated polymer matrix would result in differences in the rates of DCD migration through the polymer blends. By compounding neat and blended polymers with DCD using extrusion processing, a commercially relevant processing technology, at high loadings of 40 wt%, we can reduce formulation costs and improve commercial viability. Loadings higher than 40 wt% will most likely lead to a percolated matrix [16] and were therefore not considered.

In terms of costs, DCD typically costs ~US$1.50kg^{-1} [34], while PHBV and PCL cost ~US$6 kg^{-1} [35]. At a loading of 40 wt% DCD, the cost increases to ~US$10.50 per kg DCD applied. This presents a significant increase in unit price of DCD. However, at a typical DCD loading of 5 kg.ha^{-1} [13], this presents a cost of ~US$52.50 ha^{-1}, which is a low cost compared to the costs associated with N fertiliser losses in many farming systems. The potential cost benefit also comes from yield gains from the improved N availability, and cost effectiveness compared to controlled-release fertilisers. Optimisation of the materials would help to reduce costs of the controlled-release NI products, further supporting commercial viability.

We present here the extrusion processing conditions for the fabrication of five DCD-PHBV/PCL materials loaded DCD and with PHBV: PCL mass ratios of 1:0, 3:1, 1:1, 1:3 and 0:1. Release kinetics into water were studied under three controlled temperature conditions of 10, 23 and 40 °C, to investigate the effect of climatic conditions. This

Table 1

Molecular structure, Hildebrand solubility parameter (δ_T) and water diffusivity (D_w) for PHBV (1 % HV) and PCL (Mw 80,000 g.mol^{-1}).

Polymer	PHBV (1 %HV)	PCL
Molecular structure		
Tm (°C)	175 °C [17]	60 °C
Strain at break (%)	<5 % [17]	611 [18]
Tensile strength (MPa)	35 [17]	30 [18]
Water contact angle (°)	90.5 [23]	85 [24]
D_w (cm^2.s^{-1})	1.54×10^{-8}, at 36.5 °C[a] [19]	22.9×10^{-8}, @ 36.5 °C[a] [19]
δ_T	19.1 [25]	16.1 [26]

[a] Measured at external water vapour pressure of 0.072 atm.

temperature range was selected to provide a broad spread of temperatures across typical soil temperatures, from temperate to tropical soils, including high temperature conditions in the case of mulch films. The release kinetics were fit to a diffusion model to estimate the diffusivity of DCD through the polymer matrices. The relationship between diffusivity and temperature was used to calculate Arrhenius parameters, which allow interpolation between the studied temperatures. The produced materials are characterised through high-resolution characterisation of the pellets, including mapping the distribution of DCD, PHBV and PCL phases with Raman spectroscopy and three-dimensional density mapping through micro-computed tomography (μ-CT). Results were further supported by analysis of the crystallinity and thermal properties of the polymer blend composites and quantification of polymer chain scission through molecular weight characterisation.

2. Materials and methods

2.1. Materials

Dicyandiamide (DCD), 99 %, and polycaprolactone (PCL), with number average molecular weight (M_n) of 120,000 g.mol^{-1}, were purchased from Sigma Aldrich, Australia. The poly(3 hydroxybutyrate-*co-3*-valerate) (PHBV) with ~1 mol% HV content (as determined by ^{1}H NMR), 68 % crystallinity [36] and a weight-average molecular weight (M_w) of 590,000 g.mol^{-1} was supplied by TianAn Biopolymer, China under the trade name of ENMAT Y1000.

2.2. Extrusion processing of slow-release DCD-PHBV/PCL formulations

The PCL pellets and the DCD powder were separately pulverized using a SPEX SamplePrep Freezer/Mill™ model 6870. The ground DCD was sieved using a Retsch AS200 analytical sieve shaker (Merck), collecting material <106 μm. Five mixtures of PHBV and PCL powders were combined with PHBV:PCL mass ratios of 1:0, 3:1, 1:1, 1:3 and 0:1. The ground DCD was then mixed with the PHBV/PCL blends to produce mass loadings of 40 wt% DCD, 60 wt% polymer(s). Formulations were extruded at 180 °C using a 40/1 L/D Eurolab (Thermo-Scientific) co-rotating twin-screw extruder with a straight screw profile at 50 rpm and a 3 mm circular die. The DCD-PHBV/PCL mixtures were flood-fed into the extruder at a rate of ~5 g/min. A vent was used at Zone 8 of the extruder to remove any vapours produced. Extruded strands were pelletised with a Labtech LZ-80 Pelletiser at 10 rpm into roughly 3 × 3 mm cylindrical pellets.

2.3. Characterisation of release kinetics

2.3.1. Mobilisation of DCD from biopolymer matrices into water

The release kinetics of DCD into water from the PHBV, PHBV:PCL 3:1, 1:1 and 1:3 and PCL biopolymer matrices were monitored at temperatures of 10 °C (in a temperature-controlled refrigerator), 23 °C (room temperature, benchtop) and 40 °C (temperature-controlled, heated chamber) over 12 weeks. Five pellets (~30–40 mg each) were selected at random and photographed with a 0.5 mm graduated ruler for measuring the length and diameter of each pellet in the software ImageJ, which was required for modelling the release kinetics. The pellets were added to 50 mL of distilled water in a 70 mL plastic specimen container, with experiments conducted in triplicate. Samples (1 mL) were taken at 1 min, 30 min, 1 h, 2 h, 5 h, 10 h, 1 d, 2 d, 4 d, 7 d, 14 d, 28 d, 42 d and 56 d. DCD was quantified using ultraviolet-visible (UV–Vis) spectroscopy (see Section 2.4.1).

All five pellets from two of the three repeats were then used to quantify the DCD remaining in the pellets at the end of the experiment. The pellets were dissolved in 3 mL of chloroform at 70 °C for two to 4 h. The DCD was then extracted from this solution with 5 mL of water by vortexing the mixture for 30 s. The concentration of DCD in the water phase was then quantified using UV–Vis spectroscopy to calculate the

mass of DCD remaining in the pellets. This method has been previously shown to recover 100 ± 5 % of the expected DCD from the pellets based on the known initial loadings [15].

2.4. Analytical methods

2.4.1. Quantification of DCD

The concentration of DCD in water was quantified using UV–Vis spectroscopy. 200 μL samples were loaded into a Greiner UV Star 96 well plate and read at 230 nm with a Biotek Powerwave XS plate reader.

The absorbance of the empty plate was measured before and after loading the samples into the plate, with the absorbance of the empty plate subtracted from the measured samples. A linear calibration curve was obtained using reference solutions of between 10 and 100 mg DCD/L, with a slope of 0.022, an intercept of 0.020, an R^2 of 0.9998 and a standard error of 0.011. Following International Council on Harmonisation guidelines [37], the limit of detection (LOD) and the limit of quantification (LOQ) were estimated by multiplying the ratio of the standard error and the slope by 3.3 and 10, respectively, giving an LOD of 1.7 mg/L DCD and an LOQ of 5.24 mg/L DCD. Any samples that lay outside of range of 10–100 mg/L DCD were rerun with an appropriately adjusted dilution factor.

2.4.2. Mapping the distribution of DCD, PCL and PHBV

Raman spectroscopy was used to map DCD crystal location and investigate the blending of the PHBV and PCL polymers within the materials. The pellets were cross-sectioned using a surgical blade and mounted with Blu-Tack on a metal pill. Raman maps (30 × 30 μm, 100 × 100 pixels, 100× objective) were acquired at 50 ms integration time/pixel on an Alpha 300 Raman/AFM (WITec GmbH, Ulm, Germany), equipped with a frequency-doubled continuous-wave Nd:YAG laser to obtain a 532 nm excitation line. The stretching vibration of the CN bond in DCD at 2156 cm^{-1} was used to create the map for DCD. The PHA signal was binned around 846 cm^{-1} (-C-CH out-plane bending) vibration and PCL data was collected around the 2920 cm^{-1} CH stretching vibration. The Raman signal was processed to remove cosmic rays; the data was Savitzky-Golay smoothed and background subtracted using Project FOUR software.

2.4.3. 3-D visualization and analysis of void space

Micro-computed tomography (μ-CT) was selected to image the entire pellets in three dimensions before and after the release tests. Post-processing of the images allows estimation of the initial porosity and pore size distribution of the extruded pellets. The pellets were then scanned after eight weeks of exposure in water to investigate the change in pore distribution. The μ-CT images were acquired over 360° with a Skyscan 1272 (Skyscan, Bruker, Belgium), using an accelerating voltage of 4050 kV and a current of 200–250 mA. The following acquisition parameters were used, varying slightly depending on the X-ray transmittance through the sample: voxel size of 5–7 μm, exposure time of 150–225 ms, rotation step of 0.4°, no filter, 4 × 4 binning, and averaging of 3. NRecon Reconstruction Software (using Feldkamp algorithm) was used for reconstruction and then CTan software was used for 3-D porosity analysis (Skyscan, Bruker, Belgium).

2.4.4. Crystallinity and melting temperatures of the biopolymer blends

A differential scanning calorimeter (DSC) Q2000 (TA Instruments) under a constant nitrogen flow of 50 mL/min was used to determine the thermal properties of the neat polymers and polymer composites. Samples of 4.0 to 8.0 mg were placed in a sealed aluminium pan and were analysed using standard DSC heating and cooling scans. Each sample was heated from 25 °C to 185 °C at 10 °C/min and kept isothermal for 0.3 min, and then cooled to −10 °C at 10 °C/min. The melting temperature, T_m, and enthalpy of fusion, ΔH_m, were determined from the first heating cycle (since any slow crystallising components of PHBV blends will not crystallise in time for the second heating scan

[38]). The melt crystallisation temperature, T_{mc}, was determined from the first cooling cycle. The crystallinity of the PHBV and PCL components was estimated assuming an enthalpy of fusion of the crystalline regions of 146 J.g^{-1} and 139.5 J.g^{-1}, as determined by Barham, Keller [39] and Crescenzi, Manzini [40], respectively. Given that the HV content of PHBV was only ~1 %, the enthalpy of fusion of a theoretically 100 % crystalline PHB was appropriate in this case. For the blended materials, the crystallinity for each phase was estimated based on ratio of PHBV to PCL, accounting for the actual DCD loadings (see Table 2). Each material was run in duplicate.

2.4.5. Hydrolysis of PHBV and PCL biopolymers

Gel permeation chromatography (GPC) was used to compare the molecular weight of the biopolymer blends before and after extrusion and after release. Samples were dissolved in high performance liquid chromatography (HPLC) grade chloroform at 25 °C for 30 min for PCL and at 70 °C for 2 h for the blends containing PHBV, at a concentration of 2.5 mg/mL in a glass tube with Teflon-lined cap. An Agilent 1260 Infinity Multi Detector Suite system (Cheshire, UK) was used for the analysis, calibrated with narrowly distributed molecular weight poly-

$$\frac{M_t}{M_\infty} = At^B \ for \ 0 < t < 1 \ day \tag{1}$$

where M_t and M_∞ denote the absolute cumulative amounts of DCD released at time t, and infinite time, respectively, and A and B are constants.

The second phase of release, from Day 1 onward, was modelled based on Fick's second law of diffusion, considering both radial and axial mass transfer from a cylinder [41].

$$\frac{\partial c}{\partial t} = \frac{1}{r}\left\{\frac{\partial}{\partial r}\left(rD\frac{\partial c}{\partial r}\right) + \frac{\partial}{\partial z}\left(rD\frac{\partial c}{\partial z}\right)\right\} \tag{2}$$

where c is the concentration of DCD (mg.cm^{-3}); t is time (s); r and z represent the radial and axial coordinates relative to the centre of the pellet (cm) and D denotes the apparent diffusion coefficient (cm^2.s^{-1}).

An analytical solution to this partial differential equation for the fractional release as a function of time was derived by Vergnaud [42] as an infinite series of exponential decay terms. Fick's law is solved according to the initial and boundary conditions of initially homogeneous distribution of DCD and perfect sink conditions, giving [42]:

$$\frac{M_t}{M_\infty} = F_B + P \times \left[1 - \frac{32}{\pi^2}\sum_{n=1}^{\infty}\frac{1}{q_n^2}exp\left(-\frac{q_n^2}{R^2}\right)\sum_{p=0}^{\infty}\frac{1}{(2p-1)^2}exp\left(-\frac{(2p+1)^2\pi^2}{L^2}D(t-1)\right)\right] \tag{3}$$

styrene standards. The column set consisted of a guard column (Agilent PLgel Guard (5 μm, 7.5 mm × 50 mm)) followed by three columns in series kept at 30 °C: Agilent PLgel 105 A (5 μm, 7.5 mm × 300 mm), Agilent PLgel 103 A (5 μm, 7.5 mm × 300 mm) and Agilent PLgel 100 A (5 μm, 7.5 mm × 300 mm). A refractometer, at 30 °C, was used to quantify the biopolymers. A chloroform flow rate of 1 mL.min^{-1} was used.

2.5. Mathematical modelling of release profiles

The kinetics of DCD mobilisation from the pellets was modelled over two distinct phases of release. The release in the first day from the surface of the pellet was modelled using a power law relation:

Table 2
Summary of extrusion parameters (maximum and die temperatures (T) and torque range) and sizing (diameter, D and length, L) of the produced pellets and the actual DCD loadings. The standard deviations (±) given for D and L are based on the 15 pellets used for each material in the release studies (5 pellets for each of the three temperatures studied), while the DCD loadings are the average of 6 samples, two of each material for each temperature studied, calculated from the DCD quantified from UV–Vis spectrometry.

Material	Max./Die T (°C)	Torque (N.m)	D (mm)	L (mm)	DCD loading (wt%)
DCD-PHBV	180/160	2.5–5	3.1 ± 0.1	3.0 ± 0.2	39 ± 1 %[a]
DCD-PHBV:PCL 3:1	180/150	2.5–5	2.9 ± 0.1	2.9 ± 0.1	35 ± 1 %[b]
DCD-PHBV:PCL 1:1	180/150	2.5–5	2.9 ± 0.2	3.0 ± 0.1	30 ± 1 %[c]
DCD-PHBV:PCL 1:3	180/125	2.5–5	3.1 ± 0.4	3.0 ± 0.2	35 ± 7 %[abc]
DCD-PCL	80/60	2.5–10	2.8 ± 0.3	3.0 ± 0.3	37 ± 6 %[abc]

Nb. A multiple pairwise comparison using a repeated measures ANOVA on ranks was performed on the DCD loadings to determine their statistical groupings, shown by the superscript letters adjacent to the loading values.

where F_B is the y-intercept, introduced to account for the burst release described above; q_n are the zero order roots of the Bessel function of the first kind, and R and L are the radius and length of the cylindrical pellet (cm), respectively. For some materials, incomplete release was observed, so the parameter P was introduced to allow the theoretical plateau of the fractional release profiles to be less than unity, with a lower bound of 0.9-F_B. Parameters were estimated using Matlab R2024a software, with the first 1000 roots of the Bessel function calculated.

The temperature dependence of the Fickian diffusion coefficient was defined according to the Arrhenius rate law:

$$D = D_0 exp\left(-\frac{E_a}{RT}\right) \tag{4}$$

where D_0 (cm^2.s^{-1}) is the permeability index, E_a (J.mol^{-1}) is the activation energy of the diffusion process, R is the universal gas constant (8.3145 J.mol^{-1}.K^{-1}), and T (K) is the absolute temperature of the release experiment.

3. Results

The five PHBV/PCL blends were successfully extruded, with DCD initially mixed at 40 wt%. This shows the immediate feasibility for industrial-scale fabrication of these controlled-release nitrification inhibitor formulations. Further, this highlights the potential to encapsulate other crystalline agrichemicals in this fashion, provided they are thermally stable at the extrusion temperature (DCD is thermally stable up to ~240 °C [15]). The produced pellets were consistent in size, at roughly 3 × 3 mm length×diameter, with slightly higher variability in sizes for DCD-PCL and DCD-PHBV:PCL 1:3 (Table 2). These two materials were tackier due to the very low crystallisation temperature and the inherent characteristics of the PCL (~33 °C, see Fig. 3), which also led to higher torque during processing, see Table 2. Some DCD was lost during the fabrication process for all materials produced with some PCL content, potentially due to the higher moisture content of the cryoground PCL, or uneven DCD distribution within the extruded strand.

3.1. DCD mobilisation in water

The release of DCD into temperature-controlled water at 10 °C, 23 °C and 40 °C was monitored over 12 weeks. The mass of DCD remaining encapsulated in the pellets at the end of the 12-week experiment was also quantified by dissolving the polymer and extracting the DCD. The total mass of recovered DCD (i.e. mass of DCD in water after 12-weeks plus mass of DCD remaining in the pellet after 12 weeks) was divided by the starting mass of the pellet to calculate the DCD loading, with results shown in Table 2 for each material. There appears to be a

correlation between the amount of DCD lost from the PCL blends during processing and the die temperature, suggesting DCD might have been lost with water evaporation at the die. DCD-PHBV:PCL 1:1 had the lowest DCD contents, with 30 ± 1 wt% DCD in the produced pellets, indicating as much as 25 % of the DCD was lost during processing. The total mass of DCD recovered from each release experiment was also used to calculate the fractional release curves shown in Fig. 1.

3.1.1. Effect of matrix composition

The composition of the biopolymer controlled-release matrix had a
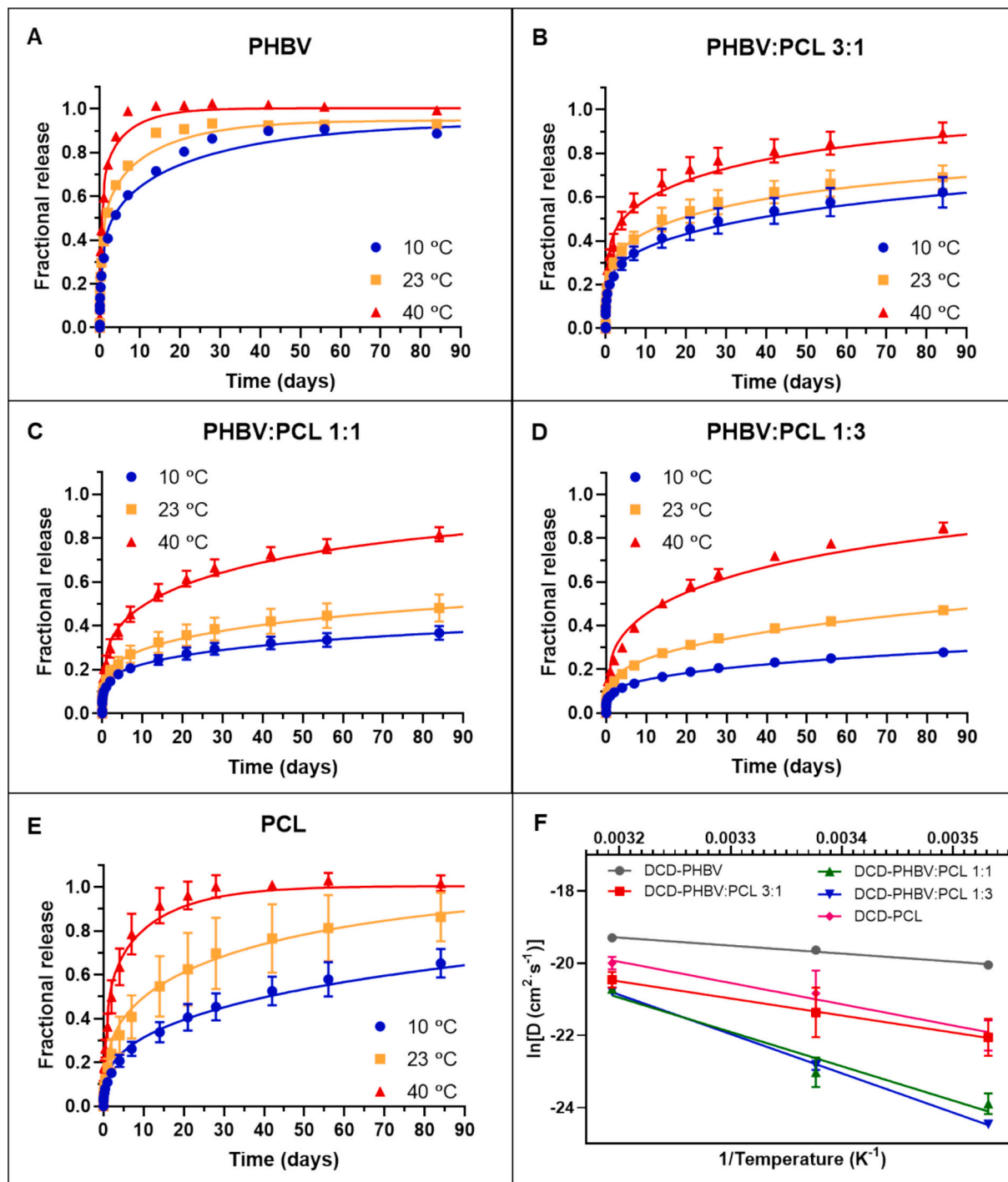

Fig. 1. Fractional release curves of DCD at 10 °C, 23 °C and 40 °C from matrices composed of (A) PHBV, (B) PHBV:PCL 3:1, (C) PHBV:PCL 1:1, (D) PHBV:PCL 1:3 and (E) PCL and (F) shows the linear regression of the Arrhenius relationship between diffusivity and temperature for each material. Error bars represent the standard deviation of the triplicate data.

significant effect on the rate of release and the amount of burst release from the surface of the pellet for most comparisons. Fig. 1 shows the release profiles for each material at each temperature condition. PHBV released the fastest out of all the materials studied, with 80 % released after 4, 10 and 20 days at 40 °C, 23 °C and 10 °C, respectively. Counterintuitively, increasing the content of the more hydrophilic PCL in the PHBV/PCL blends resulted in a slower release. In some cases, the effect of the composition of the polymer matrix was dependent on the temperature of the release media. For example, DCD-PHBV:PCL 1:1 and DCD-PHBV:PCL 1:3 released at similar rates at 23 °C and 40 °C, while at 10 °C DCD-PHBV:PCL 1:1 released significantly faster, with 37 ± 2 wt% of the DCD mobilized over the 12 week experiment compared to 28 ± 1 wt% for DCD-PHBV:PCL 1:3. DCD-PCL stands as an exception to the trend of higher PCL content slowing release. This material displayed the greatest variability for DCD mobilisation, likely because of the high porosity (Table 5) and variable loading (Table 2). DCD-PCL had a similar release profile to DCD-PHBV:PCL 3:1 at 10 °C, while at 23 °C, the fractional release was on average 17 % higher than DCD-PHBV:PCL 3:1 after 12 weeks. At 40 °C, DCD-PCL reached 80 % release within 14 days, compared to 42 days for DCD-PHBV:PCL 3:1. The release data show that the rate of release can be controlled by varying the amount of PCL in the matrix, allowing the tailoring of material design to specific applications and climate conditions. For example, at 23 °C, the fraction of DCD mobilized over 12 weeks varied from 48 ± 4 % for DCD-PHBV:PCL 1:3 to 93 % ± 1 % for DCD-PHBV, with the other materials lying between these.

The amount of DCD mobilized from the surface of the pellet can be considered as the DCD release within the first 5 h of exposure to water. Again, considering conditions at 23 °C, the amount of surface release reduces with increasing PCL content, except for 100 % PCL: reducing from 23.2 ± 0.2 % for PHBV to 15 ± 0.5 %, 10 ± 0.5 % and 8 ± 0.2 % for PHBV:PCL 3:1, 1:1 and 1:3, respectively, while PCL released 9 ± 1 %.

3.1.2. Effect of temperature on release kinetics

Increasing temperature changes the rate of diffusion processes in several ways: by increasing the kinetic energy of the DCD and water molecules; increasing chain mobility of the polymer matrices; increasing the solubility of DCD in water and in the polymer; and the equilibrium moisture content of the polymer matrices and the resulting swelling of the polymer. The effect of temperature on the fractional release of DCD from the five biopolymer matrices, with the diffusion model fits shown in Fig. 1. The modelling results for the least-squares parameter estimation are presented in Table 3. There was good agreement between the model fit and experimental data, suggesting diffusion processes likely controlled the rate of DCD mobilisation from the biopolymer matrices from one day onward. The fit parameters for the multi-phase diffusion

Table 4
Calculated Arrhenius parameters – the activation energies and pre-exponential factors.

Material	ΔE_a (kJ.mol^{-1})	D_0 (cm^2.s^{-1})
DCD-PHBV	18	5×10^{-6}
DCD-PHBV:PCL 3:1	39	4.5×10^{-3}
DCD-PHBV:PCL 1:1	79	1.25×10^{4}
DCD-PHBV:PCL 1:3	90	1.12×10^{6}
DCD-PCL	49	3.27×10^{-1}

model, A, B and D, were fit to the triplicate data sets, using the average pellet radius and length for each replicate as model inputs measured using ImageJ image processing software.

The diffusion coefficients from the best fit (Table 4) follow an Arrhenius dependence on temperature, as seen in Fig. 1F. The activation energy indicates the responsiveness of diffusivity to temperature. Temperature has the lowest effect on release from DCD-PHBV, with increasing responsiveness as the PCL content within the PHBV/PCL blends increased. This indicates that temperature has a greater impact on diffusion through the PCL dominated domains. However, DCD-PCL was an anomaly to the trend with a temperature responsiveness sitting between DCD-PHBV:PCL 3:1 and DCD-PHBV 1:1. This is an unexpected result and suggests a complex relationship between diffusivity and polymer content where multiple factors may be involved. For example, it is unclear what the effect is of having PHBV in the matrix on the temperature responsiveness of the PCL domain. Perhaps in the absence of PHBV, PCL can re-organise more easily as the matrix is exposed to warmer conditions. Further investigation is required to explore this observation to fully understand the mechanisms driven this anomaly to temperature sensitivity.

3.2. Characterisation of slow-release inhibitor formulations

To understand the observed release kinetics, each material was characterised using Raman mapping, to understand the morphology of the micro-phase separated polymer blends, DSC to determine the crystallinity of the polymers, GPC to determine the changes in molecular weight during processing and over the course of the release kinetic test in water and μ-CT to determine the porosity, pore size and pore distribution of the composites as produced and at the end of the release in water experiment.

3.2.1. The distribution of DCD, PHA and PCL

Raman mapping of each component (DCD, PHBV and PCL) allowed the visualization of the DCD crystals and the micro-phase separation
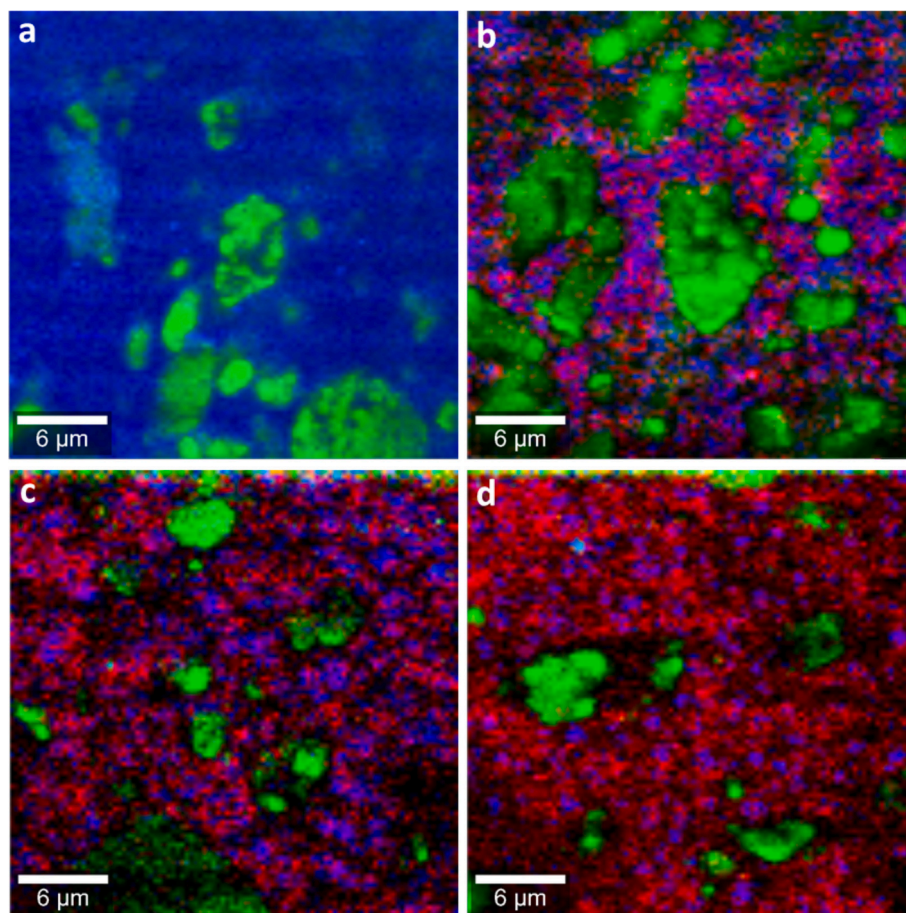
Table 3
Summary of modelling parameters from non-linear regressions of the two release stages showing the 95 % CI for each of the key fit parameters, A, B and D.

T	Material	A	B	R^2	F_B	P	D (cm.s^{-1})	R^2
10 °C	PHBV [d]	0.32 ± 0.004	0.35 ± 0.01	0.9986	0.32 ± 0.06	0.62	$(2.6 ± 0.6) \times 10^{-9}$	0.990
	PHBV:PCL 3:1 [h]	0.20 ± 0.006	0.29 ± 0.02	0.9931	0.20 ± 0.02	0.70	$(2.6 ± 0.3) \times 10^{-10}$	0.983
	PHBV:PCL 1:1 [k]	0.12 ± 0.004	0.23 ± 0.02	0.9926	0.12 ± 0.01	0.78	$(4.2 ± 0.4) \times 10^{-11}$	0.970
	PHBV:PCL 1:3 [l]	0.08 ± 0.003	0.23 ± 0.02	0.9861	0.078 ± 0.008	0.84	$(2.4 ± 0.2) \times 10^{-11}$	0.988
	PCL [i]	0.11 ± 0.005	0.38 ± 0.04	0.9815	0.11 ± 0.02	0.85	$(2.8 ± 0.3) \times 10^{-10}$	0.999
23 °C	PHBV c	0.40 ± 0.005	0.37 ± 0.02	0.9907	0.40 ± 0.03	0.60	$(3.0 ± 0.7) \times 10^{-9}$	0.971
	PHBV:PCL 3:1 [g]	0.24 ± 0.01	0.30 ± 0.03	0.9872	0.24 ± 0.03	0.66	$(5.0 ± 0.6) \times 10^{-10}$	0.991
	PHBV:PCL 1:1 [j]	0.15 ± 0.01	0.26 ± 0.04	0.9674	0.15 ± 0.03	0.75	$(1.0 ± 0.1) \times 10^{-10}$	0.972
	PHBV:PCL 1:3 [j]	0.11 ± 0.004	0.27 ± 0.02	0.9881	0.12 ± 0.01	0.78	$(1.23 ± 0.04) \times 10^{-10}$	0.989
	PCL [f]	0.18 ± 0.02	0.45 ± 0.08	0.9216	0.18 ± 0.06	0.82	$(1.1 ± 0.2) \times 10^{-9}$	0.999
40 °C	PHBV a	0.60 ± 0.02	0.35 ± 0.02	0.9936	0.60 ± 0.002	0.41	$(4 ± 2) \times 10^{-9}$	0.933
	PHBV:PCL 3:1 [e]	0.34 ± 0.02	0.31 ± 0.03	0.9811	0.34 ± 0.03	0.66	$(1.4 ± 0.2) \times 10^{-9}$	0.989
	PHBV:PCL 1:1 [f]	0.24 ± 0.02	0.26 ± 0.04	0.9565	0.23 ± 0.05	0.75	$(9.9 ± 0.3) \times 10^{-10}$	0.977
	PHBV:PCL 1:3 [f]	0.19 ± 0.01	0.33 ± 0.03	0.9826	0.19 ± 0.01	0.81	$(9.4 ± 0.5) \times 10^{-10}$	0.994
	PCL [b]	0.37 ± 0.03	0.44 ± 0.06	0.9567	0.36 ± 0.09	0.64	$(2.0 ± 0.6) \times 10^{-9}$	0.977

Superscript letters next to each material name indicate the outcomes of a multiple pairwise comparison using a repeated measures ANOVA on ranks, ranking the release curves from fastest to slowest in alphabetical order with common letter representing statistical similarity.

Fig. 2. Raman maps showing the distribution of phases separation of DCD (green), PHBV (blue) and PCL (red) in a) DCD-PHBV b) DCD-PHBV:PCL 3:1 c) DCD-PHBV:PCL 1:1 and d) DCD-PHBV:PCL 1:3 pellets.

between PHBV and PCL (Fig. 2). The size and distribution of the phases varied depending on the polymer blend. DCD-PHBV:PCL 3:1 shows PHBV and PCL are extensively intermixed such that the separate phases are hard to distinguish and appear to be co-continuous. PCL possibly exists as inclusions within the PHBV spherulites, as observed by Kim and Woo [43] and Lovera, Márquez [21] through polarizing optical microscopy. For the PHBV:PCL 1:1 and 1:3 blends, small, isolated crystals of PHBV can be visualised, but still the signal is mixed at 300 nm resolution, suggesting PCL incorporation into PHBV spherulites and vice-versa. For these two materials, the PHBV rich regions appear as isolated spherulites, held together by the continuous PCL rich phase, in part due to the higher crystallisation temperature of PHBV (Fig. 3). The size of the PHBV-rich regions reduces from ~820 ± 360 nm to 630 ± 200 nm for PHBV:PCL 1:1 and PHBV:PCL 1:3, respectively, as determined from manual measurement of 10 spherulites using the ImageJ image processing program. Unfortunately, DCD-PCL could not be imaged due to the melting of the PCL matrix under the laser. From these maps it appears the DCD crystal sizes are different for the different materials. However, these maps only capture a very small area and does not reflect the actual DCD crystal sizes. To verify this, the DCD crystals were measured by quantify the pore size distribution of the μ-CT images after release using the 3-D analysis tool with the Bruker CTAn software. The average d50 for the pores formed after DCD was released for all materials produced was 28.8 ± 8.3 μm, showing a reasonable level of consistency of encapsulated DCD particles sizes for the various materials produced.

3.2.2. Crystallinity and thermal properties of DCD-PHA/PCL composites

DSC thermograms of the first heating and first cooling cycles are shown in Fig. 3A and B, respectively. For all materials with a blend of the two polymers, there was a clear biphasic melt, indicating complete phase separation between PCL and PHBV. The PCL phase crystallised and melted at ~33 °C and ~ 60 °C, respectively. In contrast, the PHBV phase was significantly influenced by the composition of the blend. The DCD-PHBV composite showed a broad melting endotherm from ~150 to 180 °C, with two major peaks, indicating two or more PHBV crystal phases. This was potentially a result of the disruption of the crystallisation process during extrusion due to the presence of DCD crystals, leading to less perfect and/or smaller PHBV crystals. However, such multiple peaks are common for PHAs and can also be a result of physical aging, different molar mass species, different crystallite sizes, orientation effects, and so on [44]. As the PCL content increases, the width of the PHBV melting endotherm decreases, and one crystal type becomes more dominant until a single melting peak is seen for the DCD-PHBV:PCL 1:3 composite. The crystallisation temperature of the PHBV phase decreases substantially with increasing PCL content, from 107 °C for DCD-PHBV, to 80 °C for DCD-PHBV:PCL 1:3. The melting temperature of the PHBV phase was not significantly influenced by the PCL content, in line with results of Lovera, Márquez [21] for high molecular weight PCL (M_w 120,000 g.mol^{-1}) blended with PHBV, though the span of the melting temperature is reduced.

Integration of the first DSC heating scan allowed the estimation of the crystallinity of the PHBV and PCL phases. DCD-PHBV showed PHBV crystallinity of 65 %, which is comparable to reports of 68 % crystallinity by Chan, Vandi [45] who characterised ENMAT Y1000 using wide angle X-ray scattering (WAXS). For DCD-PCL, the PCL crystallinity was 65.5 %, which is higher than that reported by Blázquez-Blázquez, Pérez [46] who reported 54 % crystallinity for extruded PCL, melt pressed into
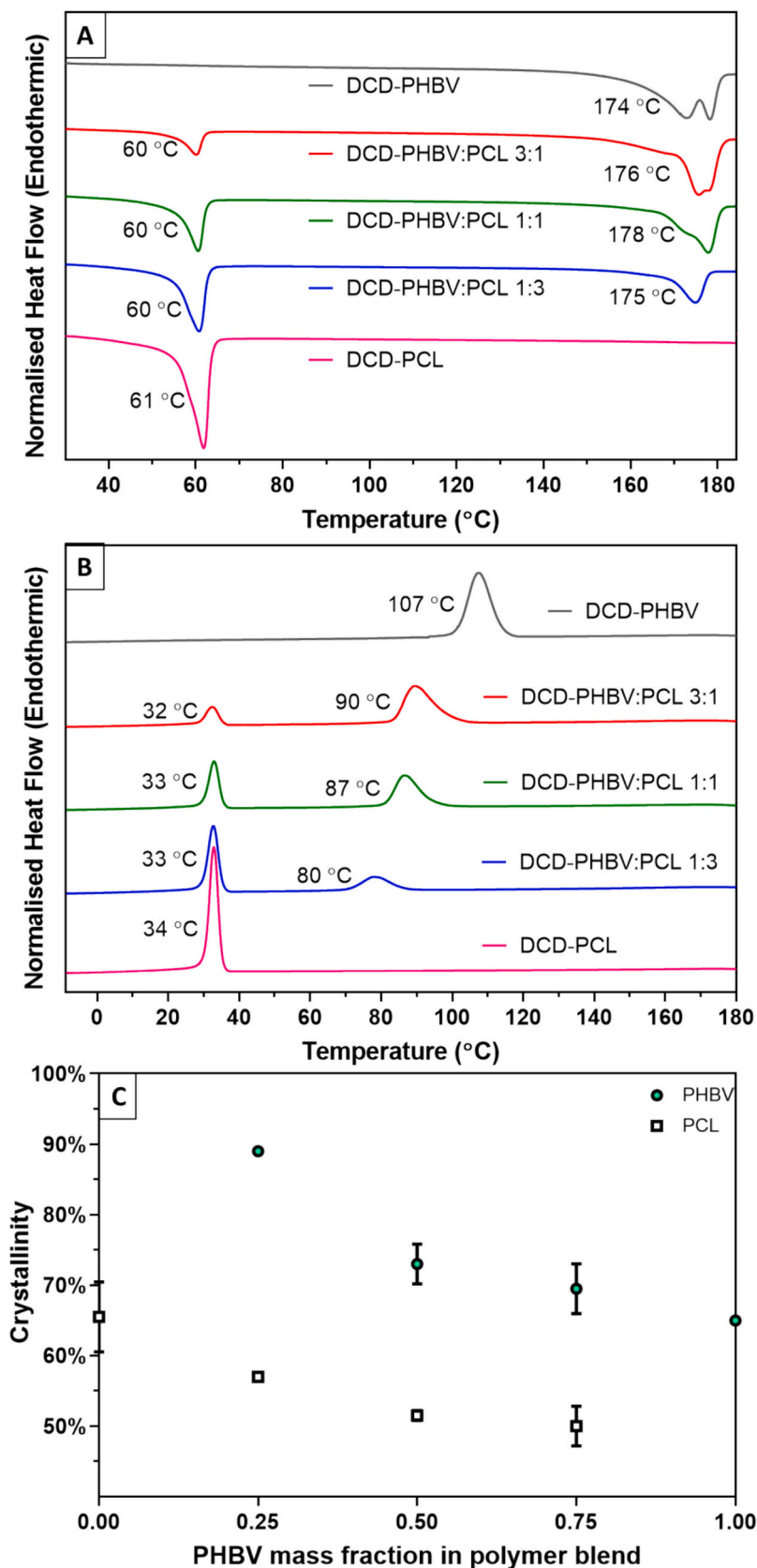
Fig. 3. (A) First heating scan and (B) first cooling scan from DSC of the extruded DCD with PHA and PCL polymer blends. The melting and crystallisation temperatures are indicated in the respective figures. (C) Crystallinity of the PHA and PCL phases as a function of the PHBV content within the polymer blend as determined from the heat of fusion for each component upon first heating, accounting for the actual DCD loadings as present in Table 2.

films.

Interestingly, as the PCL content increased, both the PHBV and the PCL phases increased in crystallinity. This was unexpected as the crystallinity of PHBV in PHBV/PCL blends has been reported to be independent of [47] or inversely correlated with [48] PCL content. However, these studies used solvent-based fabrication techniques, which will lead to co-crystallisation of the PHBV and PCL phases. The extrusion fabrication technique used here facilitates initial crystallisation of PHBV followed by the crystallisation of PCL, on cooling from the melt. At lower PHBV contents in the blend, e.g. at 25 wt% PHBV, this results in smaller spherulites that solidify first with a well-defined structure, as shown in the Raman maps (Fig. 2). Since the crystalline lamellar fibrils grow radially outward from the site of nucleation, a higher proportion of smaller spherulites results in a higher degree of crystallinity [49], at ~89 % estimated here from the DSC integration. In that same system, the lower amounts of PHBV means the matrix structure is not defined until the PCL has crystallised. This allows more freedom for the PCL phase to form more structured PCL crystallites, giving the PCL phase a higher crystallinity. Conversely, for DCD-PHBV:PCL 3:1, larger PHBV spherulites are formed first, creating more interlamellar space of amorphous polymer and therefore lower PHBV crystallinity. In this case, the higher PHBV content results in a scaffold that defines the matrix dimensions and distribution, resulting in physically confined and disrupted PCL crystallisation, with confined crystallisation known to reduce crystallinity. For example, Ho, Chiang [50] reported a reduction of PCL crystallinity of ~30 % when crystallisation was confined between lamellar microstructure of polystyrene-*b*-poly(ethylenepropylene) (PS-PEP).

The crystallisation behaviour of the polymer blends likely contributed to the observed relationship between PCL content and release kinetics. Since diffusivity through polymer crystals is significantly slower than through the amorphous domains due to tight packing of polymer chains [51], the increase in crystallinity of both polymers would have the expected impact of lower DCD diffusivity, extending the release period. Furthermore, the broad melting peak of PCL may explain the increased sensitivity of the blends with PCL to temperature.

3.2.3. Hydrolysis of the polyester chains

Gel permeation chromatography (GPC) was used to quantify molecular weights of the polymers at day 0 and day 84, allowing assessment of both the degree of polymer degradation during the extrusion process and the amount of polymer chain hydrolysis over the 12-week water release experiment. A comparison of the as-received molecular weight of the PHBV and PCL with the initial molecular weight of DCD-PHBV and DCD-PCL indicates that there was no degradation of PCL during extrusion, but significant degradation of PHBV, with a 27 ± 9 % reduction in the weight average molecular weight. This reduction in chain length did not have a significant impact on the crystallinity of the PHBV, which was determined to be 68 % crystallinity before extrusion processing by Chan, Vandi [45] using WAXS analysis and 65 % crystallinity after extrusion processing with DCD, determined from the DSC results.

The amount of hydrolysis of the polyesters over the 12-week water release experiment was negligible at 10 °C and 23 °C, while at 40 °C both pure polymers showed some reduction in molecular weight. At 40 °C,

Table 5
The porosity and pore size distribution of the extruded DCD-PHBV/PCL pellets before water immersion determined through 3D analysis of the binarised μ-CT images.

Material	Porosity (%)	d50 (μm)	Span
DCD-PHBV	9 %	22	1.3
DCD-PHBV:PCL 3:1	1 %	11	2.0
DCD-PHBV:PCL 1:1	2 %	14	1.8
DCD-PHBV:PCL 1:3	4 %	26	1.4
DCD-PCL	16 %	19	1.1

DCD-PHBV showed the most degradation, with a ~ 40 % reduction in molecular weight from the initial DCD-PHBV material. While DCD-PCL showed a 13.0 ± 0.1 % reduction in Mw. Therefore, both PHBV and PCL were susceptible to hydrolysis at 40 °C, but the rate of degradation of PHBV was higher, possibly catalyzed by the amine groups of the DCD.

3.2.4. Voids and porosity

Micro-computed tomography (μ-CT) allowed visualization and quantification of the void space distribution within the pellets in three-dimensions. Pellets imaged before release allow the quantification of the initial porosity. This initial porosity (Table 5) increases exponentially with PCL content within the blend, except for DCD-PHBV (i.e. 0 % PCL), which had a high starting porosity of 9 %. There are competing processes here, with PCL acting as a compatibiliser between DCD and PHBV, reducing porosity, while also holding more moisture prior to extrusion, which likely increases porosity in the extruded product. For DCD-PHBV: PCL 3:1 and DCD-PHBV:PCL 1:1, the starting porosity is low, existing almost exclusively near the curved surface of the pellet, which was in contact with the extruder die (see Fig. 5). Some large pores were found in the centre of DCDPHBV:PCL 1:1, but significantly more can be seen for DCD-PHBV:PCL 1:3, distributed throughout the pellet, reflected by the increase in pore size (Table 5). DCD-PCL had the highest starting porosity at 16 %, seen distributed throughout the pellet. This was surprising, since the extrusion temperature was ≤80 °C for this material. These pores may be formed by both water vapour and air pockets included into the matrix during extrusion due to the increased die pressure caused by the high viscosity and tackiness of the PCL [52].

For the pellets imaged after release, the void space represents both the starting porosity as well as the void spaces created from dissolved/released DCD crystals. For pellets where incomplete release occurred, a clear front was found between the region from which DCD had been released and the remaining core of non-dissolved DCD. This evidence supports the classical Higuchi's theory of drug release, derived assuming a sharp diffusion front [53]. In addition, these microtomographs indicate that the rate of axial diffusion is similar to that of the radial diffusion. Since the length of the pellets was roughly double the radius, the radius of the pellet therefore controls the amount of time until complete release. This will be true for all materials with length > radius, while, conversely, for materials with length < radius, the length of the pellet will control the time for complete release. Of course, the length of the pellet will still affect the shape of the curve, i.e. increasing the length of the pellet would not affect the time to complete release but would increase the time to 50 % and 80 % release.

The porosity of the pellets before and after release in water was analysed using the Bruker CTAn 3D analysis tools. Results for the open and closed porosity estimates from the binarized images are summarised in Fig. 6. By comparing the porosity before and after release, we could estimate the percentage of DCD release from the porosity data. Generally, the increase in porosity observed in the μ-CT aligned with the fractional release of DCD determined from the water release study (shown in the bottom right of each μ-CT slice within Fig. 5). However, in some cases they did not. For example, for DCD-PCL at 10 °C, the μ-CT images indicate ~40 % release compared to 72 % release calculated from the solution concentrations for that replicate. At 40 °C, the fractional release of DCD was found to be ~85 % for DCD-PHBV:PCL 3:1, 1:1 and 1:3, while the μ-CT show ~100 %, ~85 % and ~ 98 % release, respectively (calculated based on the volume of the remaining undissolved core compared to the total volume of the pellet). These discrepancies likely result from pellet-to-pellet variability, since the solution data is an average of the five pellets in each container. This variability could result from differences in: i) pellet heights and diameters; ii) starting porosities of individual pellets; or iii) DCD loadings. This will also be some randomness in the distribution of DCD, PHBV and PCL phases within the pellet.

The porosity results should be treated with caution, due to the limited resolution of this μ-CT technique that relies on manual

thresholding for the binarization. As such, the exact degree of open versus closed porosity cannot be determined with certainty. However, there is a clear difference in the degree of closed porosity between the materials with PCL in them compared to the DCD-PHBV. This suggests that those polymer blends interact more with the DCD, wrapping around individual crystals, while for DCD-PHBV there was likely a connected network of DCD crystals within the matrix.

4. Discussion

The observed decrease in release kinetics observed as the proportion of PCL increased was unexpected. With the water permeability of PCL being some 15 times higher than that of PHBV (Table 1), we expected the release to increase with increasing PCL content. The characterisation of the materials provided evidence which helps to understand this counter-intuitive observation, and the release mechanism and fundamental knowledge gained from this work are discussed below.

4.1. Mechanisms controlling mobilisation and interpretation of "diffusivity"

The counter-intuitive release kinetic observation is likely a product of the differences in the nature of the pathway the DCD travels as it migrates to the surface of the pellet. In the case of DCD-PHBV, it is likely that the DCD did not diffuse through layers of PHBV. Rather, it seems that the DCD crystals existed in the matrix as a connected network, as described by Levett, Donose [16], and the rate-limiting step is likely the diffusion of DCD along a tortuous path within the PHBV matrix, created by the pores and voids formed as DCD crystals dissolved. In this case, the apparent diffusivity reported represents a lumped parameter of the tortuosity (τ) and the diffusivity of DCD in water.

Interestingly, the plateau of the fractional release from a PHBV matrix was dependent on temperature. At 10 °C, 23 °C and 40 °C the plateau was 90 %, 91 % and 100 %, respectively. This correlates with the amount of PHBV degradation, with 0 %, 6 ± 2 % and 39 ± 2 % reduction in molecular weight after 12 weeks (Fig. 4). Hydrolysis of PHBV chains can cause microscopic changes in the matrix structure, opening channels, such as cracks, as reported by Levett, Donose [54], or provides more free space and/or voids between the polymer chains since the lower molecular weight fractions have more mobility. This enables increased internal water access, accelerating the release of the previously inaccessible fraction of DCD. Hydrolytic degradation of PHBV was unexpected under these abiotic conditions. However, since DCD has three amine groups, this may be evidence of base catalyzed hydrolysis of the ester linkages in both PHBV and PCL.

Addition of PCL to the PHBV appears to reduce the connectivity between adjacent DCD crystals. For DCD-PHBV:PCL 3:1, the mechanism controlling DCD release is likely a combination of DCD diffusion through water along a tortuous path within the matrix, and diffusion through thin layers of PCL. Adding more PCL into the blend likely increased the thickness of the PCL layer through which the DCD diffused, slowing the rate of DCD release. For DCD-PCL, the higher starting porosity means the path for DCD release will occur through diffusion through thin layers of PCL and the more rapid diffusion of DCD through water-filled pores. Intriguingly, DCDPHBV:PCL 1:1 and 1:3 released at similar rates, particularly at 23 °C and 40 °C. The characterisation of these materials suggests competing processes influence the release kinetics. Following the theory proposed above, the higher PCL content of DCD-PHBV:PCL 1:3 should result in thicker layers of PCL for DCD to diffuse through. Furthermore, DSC results indicated that both the PCL and the PHBV phases had a higher degree of crystallinity, which slows diffusion [51]. However, the µ-CT results show a higher starting porosity for this material, which accelerates release. In addition, the DCD loading for DCD-PHBV:PCL 1:3 was ~12 % higher than DCD-PHBV:PCL 1:1. The significantly faster release from DCD-PCL pellets over DCD-PHBV:PCL 1:1 and DCD-PHBV:PCL 1:3 is certainly related to the much higher initial porosity of this material. However, the incorporation of PHBV in the blends will result in a more hydrophobic matrix [55], which may be responsible for the lower diffusivities seen in the blends compared to DCD-PCL.

Following the proposed theory, it is reasonable that the blends with higher PCL contents showed the highest dependence on temperature. The diffusion of DCD through the layers of PCL will be more dependent on temperature, compared to the diffusion of DCD through water. This can be explained by the multi-factorial effect of increased temperature, affecting:

  i) the rate of diffusion of water in the polymer matrix, due to increase kinetic energy of water and polymer chain mobility
 ii) the rate of DCD dissolution, likely related to or limited by the rate of DCD diffusion away from DCD crystals, and
iii) the rate of DCD diffusion in water, due to higher kinetic energy of the DCD molecules
 iv) the rate of DCD diffusion back through the biopolymers, due to higher kinetic energy of the DCD molecules and increased polymer chain mobility
  v) the solubility of DCD within the biopolymers and in water
 vi) the rate of desorption of DCD off the polymer and into the water phase
vii) the rate of hydrolysis of ester linkages in the PHBV and PCL (as evidenced from the GPC results, Fig. 4).

For materials where DCD diffuses through layers of PCL, all the above are relevant and effected by temperature. Whereas, for DCD-PHBV, where DCD diffuses along a tortuous path of water filled channels, only ii) and iv) are relevant.

In a field environment, soil microbes will metabolise both PHBV and PCL as a carbon source [14]. Both polymers degrade via an enzymatic surface erosion mechanism, while PCL also undergoes abiotic hydrolysis through the bulk of the material. Our previous study [15], showed for a material with 25 wt% DCD in PHBV, biodegradation of the PHBV matrix accelerated release into soil from ~28 days onward. The rate of polymer degradation in soil is a complex parameter that depends largely on the soil type, pH, texture, microbial population present, soil moisture content and temperature [15,56]. Surface erosion of the polymers will likely open pathways for encapsulated DCD and reduce the diffusion path length, while the bulk hydrolysis of PCL would accelerate the rate of diffusion through the matrix. Further investigation would improve our understanding on the role of degradation on release from matrices composed of PHBV/PCL blends and how biodegradation can be
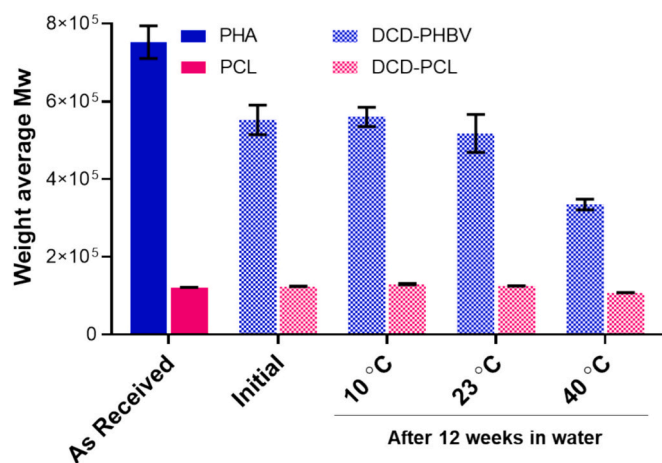

Fig. 4. GPC results showing the weight average molecular weight (Mw) of PHBV and PCL as received (before extrusion), after extrusion with DCD (initial) and after the 12-week water release experiments at 10 °C, 23 °C and 40 °C.
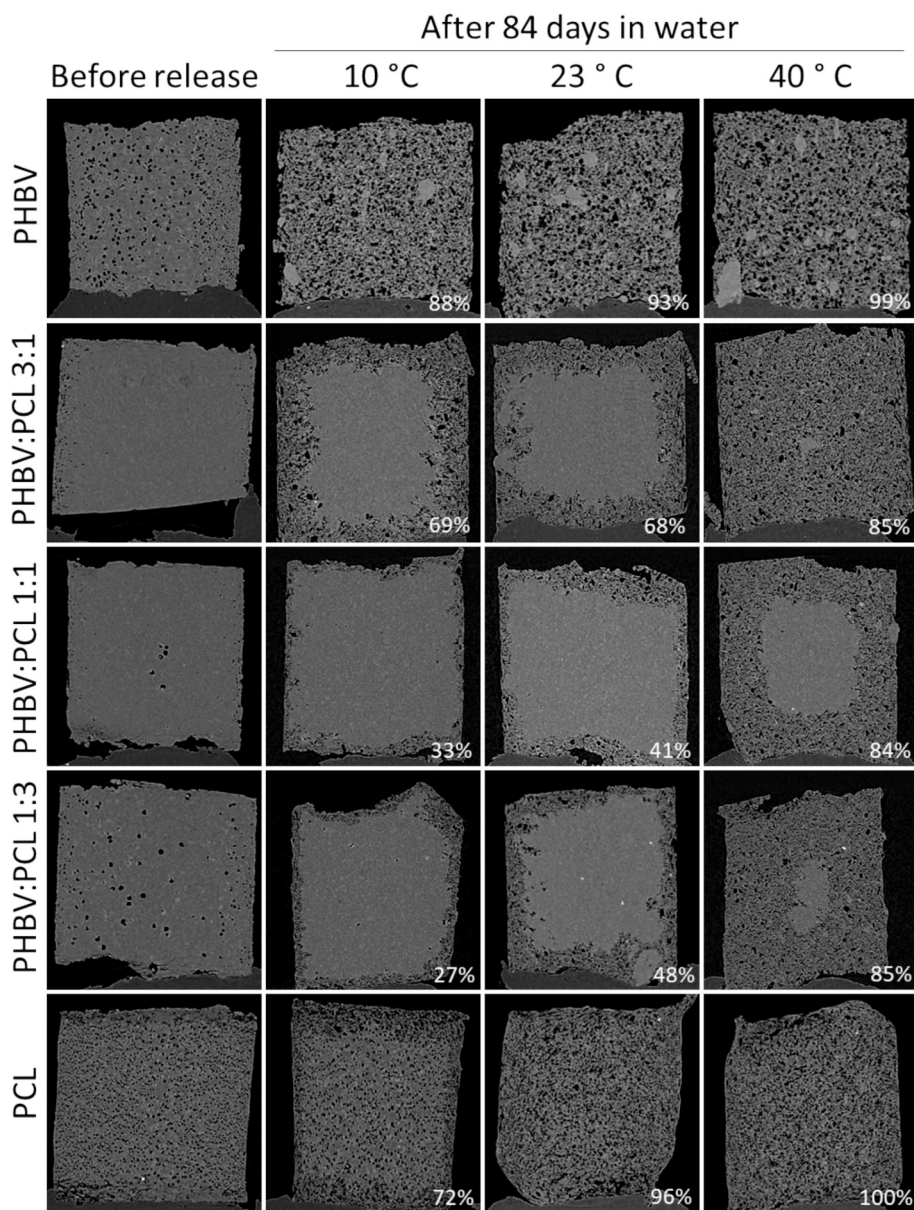
Fig. 5. Coronal μ-CT slices of DCD-PHBV/PCL pellets scanned after extrusion and after release in water for 84 days at 10 °C, 23 °C and 40 °C. Cumulative percentage of DCD release in water calculated from the UV–Vis absorption data are shown in bottom right corner of each image.

controlled to minimize its impact on release kinetics over the target release period. In addition, soil parameters impact the performance of nitrification inhibitors, affecting factors such as rates of inhibitor migration through the soil and rates of inhibitor degradation.

4.2. The importance of polymer-agent affinity

The counter-intuitive correlation between release kinetics and the hydrophobicity of the matrix may be explained by the increased affinity of DCD to PCL over PHBV. The interaction between DCD and the polymer matrix occurs during extrusion processing and the subsequent crystallisation of the matrix. If the polymer-DCD interaction is weak, it is more likely that the polymer will pull away during the crystallisation process, leaving voids and channels for direct water access to the DCD within the matrix, which is supported by the high degree of open porosity estimated from the μ-CT images of the DCD-PHBV pellet after release. In contrast, if a stronger interaction exists, contact between the DCD crystals and the polymer matrix minimizes the formation of voids

and as a result forces DCD to diffuse through layers of polymer along the release pathway, again supported by the increase of closed porosity observed in the PCL blends after release in water.

DCD is a water-soluble compound which contains several polar functional groups - most notably amino groups and a nitrile group. The presence of these groups allows DCD to form hydrogen bonds and interact strongly with water molecules, facilitating dissolution. Similarly, the degree of interaction between DCD and the polymer will depend on the ability to form hydrogen bonds. The lower Hildebrand parameter of PCL (Table 1) is a good indicator that it is more likely to interact with water soluble compounds such as DCD. Another measure of a polymer's ability to form hydrogen bonds is water contact angle. A higher degree of hydrogen bonding between the surface of the polymer and the water droplet causes the droplet to spread out, lowering the contact angle. PCL has been reported to have a contact angle of 85° [19], slightly lower than that of PHBV at 90° [18]. While these are comparable contact angles, it should be noted that water contact angle is a surface phenomenon of a solid and may not strongly correlate with interactions
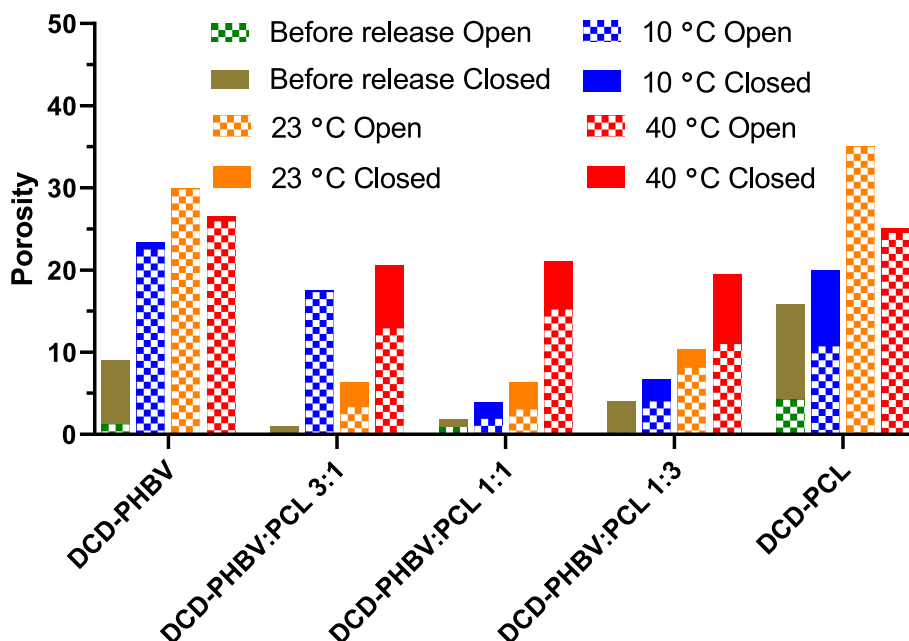
Fig. 6. Summary of the porosity results from the 3D porosity analysis conducted using the Bruker CTAn software.

that form in the bulk of the materials in the melt and during the crystallisation process. It should be further noted that the DCD will more readily interact with the more mobile amorphous chains within a semi-crystalline polymer. Given that PHBV had higher crystallinity than PCL in each of the blended formulations, this will also affect both the free volume available as well as the extent of interaction of DCD with the polymer. Further investigation into the affinity and interaction between the polymers and the DCD is required to explore this concept further.

4.3. Material design for tailoring release

This work uses DCD as a model water-soluble crystalline material. However, the knowledge gained here could likely be applied to the encapsulation of most water-soluble crystalline agrichemicals. These results show the rate of release of a crystalline agrichemical can be tailored to the climatic conditions and crop or soil-specific requirements, bearing in mind that the relative affinity of different chemicals for the different polymer matrixes will likely affect the relative release rates. Take the example of moderate soil temperatures around 23 °C. If 50 % release is desired within the first week, month or 3 months, the recommended polymer matrix would be PHBV, PHBV:PCL 3:1, or PHBV: PCL 1:1, respectively. Alternatively, if the rate of DCD degradation was known for a specific soil in a specific climate, the modelling results presented here could be used to determine which material would sustain an active concentration of DCD within the soil profile for the longest amount of time. This tailoring of release kinetics is pertinent to the effective delivery of agrichemicals and minimization of harmful environmental losses. It is hypothesized that delivering NIs slowly into the soil will improve their ability to inhibit nitrifying microorganisms, holding the N as NH_4^+ for longer, thereby reducing NO_3^-/NO_2^- leaching and denitrification to N_2O, with the potential drawback of higher NH_3 emissions. Further pot and field-based studies are needed to test this hypothesis.

Although increasing PCL content of the polymer blend from 0 to 50 wt% led to a significant reduction in release kinetics, increasing the PCL content further, from 50 to 75 wt%, had no effect at 23 °C and 40 °C. This shows a limitation of the extent to which the polymer ratio has a marked impact on release kinetics and highlights a need to investigate if the release kinetics can be "fine-tuned" using smaller differences in blend composition between 0 and 50 wt% PCL.

5. Conclusion

Nitrification inhibitors (NIs), such as dicyandiamide (DCD), hold great potential in reducing N losses from agricultural systems to the environment. However, the relatively rapid degradation of DCD in soil limits its effectiveness, particularly in the tropics. This work presents a simple and effective method to encapsulate and protect the DCD from degradation by extruding the DCD with biodegradable polymers to form controlled-release DCD pellets. These pellets show the potential to release the DCD over many months. By blending two polymers with differing water barrier properties the release rate could be tailored for specific soil types and climatic conditions, with release ranging from 80 % release in ~10 days at 23 °C down to <50 % release in 84 days depending on the matrix composition. Interestingly, the more hydrophobic PHBV matrix released DCD the fastest and release kinetics slowed as the more hydrophilic PCL content increased. Additionally, by studying release at multiple temperatures the Arrhenius parameters could be estimated, allowing estimation of release kinetics at any temperature condition. Further work is required to understand the influence of polymer degradation on release rates and pot trials to determine the effectiveness of these controlled release formulations on limiting nitrification for longer periods over DCD alone.

CRediT authorship contribution statement

Ian Levett: Writing – review & editing, Writing – original draft, Visualization, Validation, Project administration, Methodology, Investigation, Formal analysis, Data curation, Conceptualization. **Minjie Liao:** Writing – original draft, Formal analysis, Data curation, Conceptualization. **Chris Pratt:** Writing – review & editing, Supervision, Methodology, Funding acquisition, Formal analysis, Conceptualization. **Matthew Redding:** Writing – review & editing, Supervision, Methodology, Funding acquisition, Formal analysis, Conceptualization. **Steven Pratt:** Writing – review & editing, Visualization, Supervision, Resources, Project administration, Methodology, Investigation, Funding acquisition, Formal analysis, Conceptualization. **Bronwyn Laycock:** Writing – review & editing, Visualization, Supervision, Resources, Project administration, Methodology, Investigation, Funding acquisition, Formal analysis, Data curation, Conceptualization.

Declaration of competing interest

Acknowledgements

Data availability

Data will be made available on request.

References

[1] W. Steffen, et al., Planetary boundaries: guiding human development on a changing planet, Science 347 (6223) (2015).
[2] C. Qiao, et al., How inhibiting nitrification affects nitrogen cycle and reduces environmental impacts of anthropogenic nitrogen input, Glob. Chang. Biol. 21 (3) (2015) 1249–1257.
[3] C. Liu, K. Wang, X. Zheng, Effects of nitrification inhibitors (DCD and DMPP) on nitrous oxide emission, crop yield and nitrogen uptake in a wheat–maize cropping system, Biogeosciences 10 (4) (2013) 2427–2437.
[4] M. Yang, et al., Efficiency of two nitrification inhibitors (dicyandiamide and 3, 4-dimethypyrazole phosphate) on soil nitrogen transformations and plant productivity: a meta-analysis, Sci. Rep. 6 (2016), p. 22075.
[5] D. Abalos, et al., Meta-analysis of the effect of urease and nitrification inhibitors on crop productivity and nitrogen use efficiency, Agr Ecosyst Environ 189 (2014) 136–144.
[6] R. Prasad, J.F. Power, Nitrification inhibitors for agriculture, health, and the environment, Adv. Agron. 54 (1995) 233–281.
[7] K.F. Bronson, J.T. Touchton, R.D. Hauck, Decomposition rate of dicyandiamide and nitrification inhibition, Commun. Soil Sci. Plant Anal. 20 (19–20) (1989) 2067–2078.
[8] E.S. Papadopoulou, et al., The effects of Quinone imine, a new potent nitrification inhibitor, dicyandiamide, and Nitrapyrin on target and off-target soil microbiota, Microbiology Spectrum 10 (4) (2022) p. e02403-21.
[9] J. Cayzer, et al., Systemic granulomatous disease in dairy cattle during a dicyandiamide feeding trial, N. Z. Vet. J. 66 (2) (2018) 108–113.
[10] R.K. Salis, et al., Multiple-stressor effects of dicyandiamide (DCD) and agricultural stressors on trait-based responses of stream benthic algal communities, Sci. Total Environ. 693 (2019) 133305.
[11] X.M.B. Macadam, et al., Dicyandiamide and 3,4-dimethyl pyrazole phosphate decrease N2O emissions from grassland but dicyandiamide produces deleterious effects in clover, J. Plant Physiol. 160 (12) (2003) 1517–1523.
[12] F.M. Kelliher, et al., The temperature dependence of dicyandiamide (DCD) degradation in soils: a data synthesis, Soil Biol. Biochem. 40 (7) (2008) 1878–1882.
[13] M.E. Trenkle, Slow- and Controlled-Release and Stabilized Fertilizers: An Option for Enhancing Nutrient Efficiency in Agriculture, International Fertilizer Industry Association, Paris, France, 2010.
[14] B. Laycock, et al., Lifetime prediction of biodegradable polymers, Prog. Polym. Sci. 71 (2017) 144–189.
[15] I. Levett, et al., Understanding the mobilization of a nitrification inhibitor from novel slow release pellets, fabricated through extrusion processing with PHBV biopolymer, J. Agric. Food Chem. 67 (9) (2019) 2449–2458.
[16] I. Levett, et al., Designing for effective controlled release in agricultural products: new insights into the complex nature of the polymer–active agent relationship and implications for use, J. Sci. Food Agric. 100 (2020) 4723–4733.
[17] B. Laycock, et al., The chemomechanical properties of microbial polyhydroxyalkanoates, Prog. Polym. Sci. 38 (3) (2013) 536–583.
[18] M. Przybysz, et al., Structural and Thermo-mechanical properties of poly (ε-caprolactone) modified by various peroxide initiators, Polymers (Basel) 11 (7) (2019).
[19] J.-S. Yoon, et al., Diffusion coefficient and equilibrium solubility of water molecules in biodegradable polymers, J. Appl. Polym. Sci. 77 (8) (2000) 1716–1722.
[20] Z. Qiu, et al., Miscibility and crystallization behavior of biodegradable blends of two aliphatic polyesters. Poly(3-hydroxybutyrate-co-hydroxyvalerate) and poly (ε-caprolactone), Polymer 46 (25) (2005) 11814–11819.
[21] D. Lovera, et al., Crystallization, morphology, and enzymatic degradation of Polyhydroxybutyrate/Polycaprolactone (PHB/PCL) blends, Macromol. Chem. Phys. 208 (9) (2007) 924–937.
[22] E. Moll, A. Chiralt, Improving Thermo-sealing of poly(3-hydroxybutyrate-co-3-hydroxyvalerate) by blending with Polycaprolactone, Polymers 16 (23) (2024) 3255.
[23] Y.J. Chae, T.G. Lee, Controlled biodegradability of polyhydroxybutyrate via surface coating with cellulose triacetate, Sci. Rep. 15 (1) (2025), p. 25776.
[24] Z.G. Tang, et al., Surface properties and biocompatibility of solvent-cast poly [ε-caprolactone] films, Biomaterials 25 (19) (2004) 4741–4748.
[25] M. Terada, R.H. Marchessault, Determination of solubility parameters for poly(3-hydroxyalkanoates), Int. J. Biol. Macromol. 25 (1) (1999) 207–215.
[26] K. Adamska, A. Voelkel, A. Berlińska, The solubility parameter for biomedical polymers—application of inverse gas chromatography, J. Pharm. Biomed. Anal. 127 (Supplement C) (2016) 202–206.
[27] A.N. Boyandin, et al., Constructing slow-release formulations of ammonium nitrate fertilizer based on degradable poly(3-hydroxybutyrate), J. Agric. Food Chem. 65 (32) (2017) 6745–6752.
[28] A.N. Boyandin, et al., Constructing slow-release formulations of Metribuzin based on degradable poly(3-hydroxybutyrate), J. Agric. Food Chem. 64 (28) (2016) 5625–5632.
[29] J. Suave, et al., Biodegradable microspheres of poly(3-hydroxybutyrate)/poly (ε-caprolactone) loaded with malathion pesticide: preparation, characterization, and in vitro controlled release testing, J. Appl. Polym. Sci. 117 (6) (2010) 3419–3427.
[30] F.M. Barboza, et al., PCL/PHBV microparticles as innovative carriers for Oral controlled release of Manidipine Dihydrochloride, Scientific World Journal 2014 (2014) 10.
[31] M.K. Riekes, et al., Evaluation of oral carvedilol microparticles prepared by simple emulsion technique using poly(3-hydroxybutyrate-co-3-hydroxyvalerate) and polycaprolactone as polymers, Mater. Sci. Eng. C 31 (5) (2011) 962–968.
[32] J.B.E. Mendes, et al., PHBV/PCL microparticles for controlled release of resveratrol: physicochemical characterization, antioxidant potential, and effect on hemolysis of human erythrocytes, TheScientificWorldJournal 2012 (2012) 542937–542950.
[34] echemi.com, Dicyandiamide China Regional Price, 2025. Available from: https://www.echemi.com/pmp/dicyanodiamide-pid_Seven32758.html.
[35] I. Levett, et al., A new tool to screen biodegradable polymers as technically and commercially viable fertiliser coatings, Sci. Total Environ. 976 (2025) 179371.
[36] C.M. Chan, et al., Understanding the effect of copolymer content on the processability and mechanical properties of polyhydroxyalkanoate (PHA)/wood composites, Applied Science and Manufacturing 124 (2019) 105437–105447.
[37] A. Teasdale, R.W. Nims, D. Elder, Q2(R1) Validation of Analytical Procedures: Text and Methodology, John Wiley & Sons, Incorporated, United States, 2017.
[38] B. Laycock, et al., Crystallisation and fractionation of selected polyhydroxyalkanoates produced from mixed cultures, N. Biotechnol. 31 (4) (2014) 345–356.
[39] P.J. Barham, et al., Crystallization and morphology of a bacterial thermoplastic: poly-3-hydroxybutyrate, J. Mater. Sci. 19 (9) (1984) 2781–2794.
[40] V. Crescenzi, et al., Thermodynamics of fusion of poly-β-propiolactone and poly-ε-caprolactone. comparative analysis of the melting of aliphatic polylactone and polyester chains, Eur. Polym. J. 8 (3) (1972) 449–463.
[41] J. Crank, The Mathematics of Diffusion, 2nd ed., Clarendon Press, Oxford, Eng, 1975.
[42] J.M. Vergnaud, in: ProQuest (Ed.), Controlled Drug Release of Oral Dosage Forms, E. Horwood, New York, 1993.
[43] B.O. Kim, S.I. Woo, Compatibilizing capability of poly(β-hydroxybutyrate-,co-ε-caprolactone) in the blend of poly(β-hydroxybutyrate) and poly(ε-caprolactone), Polym. Bull. 41 (6) (1998) 707–712.
[44] N. Yoshie, Y. Inoue, Cocrystallization and phase segregation in blends of two bacterial polyesters, Macromol. Symp. 224 (1) (2005) 59–70.
[45] C.M. Chan, et al., Understanding the effect of copolymer content on the processability and mechanical properties of polyhydroxyalkanoate (PHA)/wood composites, Compos. A: Appl. Manuf. 124 (2019) 105437.
[46] E. Blázquez-Blázquez, et al., Crystalline characteristics and their influence in the mechanical performance in poly(ε-Caprolactone) / high density polyethylene blends, Polymers 11 (11) (2019) 1874.
[47] Y.S. Chun, W.N. Kim, Thermal properties of poly(hydroxybutyrate-co-hydroxyvalerate) and poly(ε-caprolactone) blends, Polymer 41 (6) (2000) 2305–2308.
[48] V. Chiono, et al., Poly(3-hydroxybutyrate-co-3-hydroxyvalerate)/poly (ε-caprolactone) blends for tissue engineering applications in the form of hollow fibers, J. Biomed. Mater. Res. A 85A (4) (2008) 938–953.
[49] C. Dingler, K. Dirnberger, S. Ludwigs, Semiconducting polymer Spherulites—from fundamentals to polymer electronics, Macromol. Rapid Commun. 40 (1) (2019), p. 1800601.

[50] R.-M. Ho, et al., Crystallization and melting behavior of poly(ε-caprolactone) under physical confinement, Macromolecules 38 (11) (2005) 4769–4779.

[51] W.R. Vieth, Diffusion in and through Polymers: Principles and Applications, Hanser, Munich New York, 1991.

[52] C. Saldanha do Carmo, et al., The impact of extrusion parameters on physicochemical, nutritional and sensorial properties of expanded snacks from pea and oat fractions, LWT 112 (2019) 108252.

[53] T. Higuchi, Rate of release of medicaments from ointment bases containing drugs in suspension, J. Pharm. Sci. 50 (10) (1961) 874–875.

[54] I. Levett, et al., High-resolution μ-CT Reveals Crazing In A Hydrophobic Composite - A New Mechanism for Mobilization In Controlled Release Applications, In press, 2020.

[55] H. Liu, et al., Blending modification of PHBV/PCL and its biodegradation by Pseudomonas mendocina, J. Polym. Environ. 25 (2) (2017) 156–164.

[56] A.N. Boyandin, et al., Microbial degradation of polyhydroxyalkanoates in tropical soils, Int. Biodeter. Biodegr. 83 (2013) 77–84.